WCTE 2016
World Conference on Timber Engineering
August 22-25, 2016 | Vienna, Austria

MECHANICAL PROPERTIES OF CROSS-LAMINATED TIMBER ACCOUNTING FOR NON-BONDED EDGES AND ADDITIONAL CRACKS

John A. Nairn[1]

ABSTRACT: Cross-laminated timber (or CLT) must be recognized as a "precracked" wood composite material where the non-bonded edges within each layer act as cracks in the structure. Furthermore, differential shrinkage between the layers of installed CLT panels subjected to variations in moisture and temperature will result in additional cracks forming parallel to the initial precracks. Fortunately, there is a large literature on the effect of such cracks in cross-laminated composites used in aerospace composites. This paper applies prior literature (when available), and extends it (when needed) to derive all mechanical, thermal expansion, and moisture expansion properties of CLT as s function of the number of cracks in each layer. These results can be used to better design CLT structures. Furthermore, because CLT will form additional cracks when in service, these equations should be a key component of any durability analysis.

KEYWORDS: Cross Laminated Timber, Mechanical Properties, Thermal Expansion, Moisture Expansion, Durability

1 INTRODUCTION

Cross laminated timber (CLT) is made by laminating three or more layers of timber such that the grain directions in alternate layers are at right angles to each other much like the grain directions in the veneer layers of plywood. Glue is applied between the layers on the faces of the timber, but no glue is applied on timber edges within each layer. CLT must therefore be recognized as a precracked composite where the timber edges represent periodic "precracks" in every layer. Furthermore, CLT will develop more cracks over time due to environmental exposure and differential layer shrinkages. For example, figure 1 shows a CLT structure on display in the lobby of the College of Forestry at Oregon State University illustrating both "precracks" (non-bonded edges) and "added cracks" (within timber elements). Those involved in wood construction are used to seeing cracks in solid-sawn lumber and glulam, but the structure of CLT causes the driving force for formation of such cracks to be much greater [1-4] and the consequences of those cracks to be more severe [5-7]. Attempts to ameliorate effects of precracks by applying glue to the edges would be thwarted by natural formation of added cracks over time.

The inescapable conclusions are that CLT structures must be designed with tools that recognize cracks and durability analysis of CLT must account for the rate of formation of added cracks and their role in changing the properties of the structure. Fortunately, the analysis of CLT need not re-invent the tools because many of the needed methods

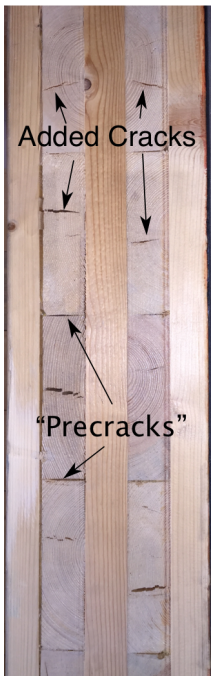

***Figure 1**: Typical CLT has "precracks" (initial non-glued edges) and "added cracks" induced by environment.*

are already available from prior research on cross-ply laminates made with carbon fibre or glass fibre materials. Applications of synthetic cross-ply laminates include bicycle tubes and ski poles. Common applications that are

[1] John A. Nairn, Oregon State University, Corvallis, OR USA, John.nairn@oregonstate.edu

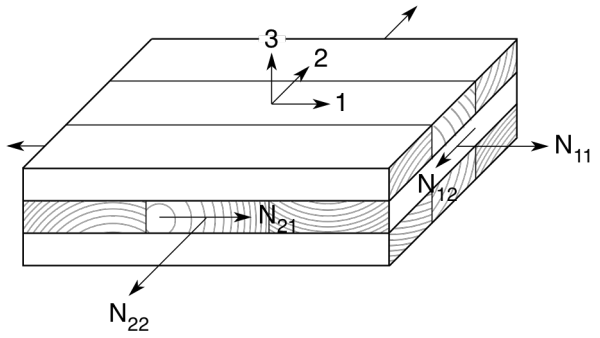

***Figure 2**: A three-layer CLT panel where 1, 2, and 3 refer to laminate directions and N_{ij} refer for force per unit length (force resultants) applied to the laminate.*

close to cross-ply laminates include filament wound pressure vessels and fibreglass pipes. Unlike CLT, synthetic cross-ply laminates are not manufactured with precracks (non-glued edges), but like CLT, laminates are prone to added cracks (known as "microcracks" or "transverse cracks") caused by mechanical loads or by residual stresses. The consequences of microcracks are a reduction in laminate properties and a promotion of more serious damage such as delamination. The linking of microcracks and delaminations can lead to leakage in pressure vessels or pipes that represent functional failure despite only modest changes in mechanical properties [8].

The analysis of microcrack formation in cross-ply laminates has focused on energy methods where the next crack forms when the energy release rate for formation of the next microcrack exceeds the toughness of the ply material [1-4]. A prerequisite to finding this energy release rate is a mechanics analysis for the mechanical and expansion properties of the laminate as a function of the number of microcracks [1-7]. Although most prior microcracking models have been 2D models for cracking in a single layer, Hashin analysed a three-layer, cross-laminated composite with orthogonal cracks in all layers [6]. This paper applies and extends Hashin's variational mechanics methods to find in-plane moduli, Poisson's ratio, and thermal and moisture expansion coefficients of CLT, all as a function of crack spacings in the layers. The use of these results for evaluating the driving forces for formation of additional cracks is briefly discussed.

2 THEORY

The most relevant paper for analysis of CLT is Hashin's 3D analysis of an orthogonally cracked laminate [6]. From a mechanics point of view, Hashin's paper analysed the CLT panel shown in figure 2, and completed that analysis before CLT was developed as a product. Hashin's solved for modulus in the laminate 1 direction (due to load N_1) and for Poisson's ratio (ν_{12}) for a laminate with transversely isotropic plies with fibre direction defining the axial direction. This section applies his methods to include orthotropic properties of wood for the layers, to additionally determine properties for loading in the laminate 2 direction (due to load N_2), and to give a corrected Poisson's ratio.

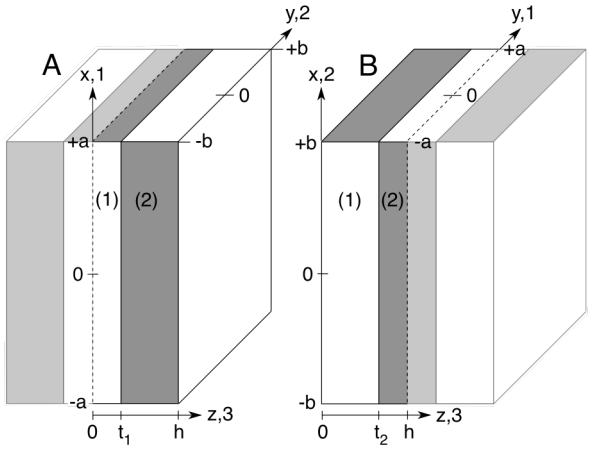

***Figure 3**: Unit cell for analysis of CLT properties. The shaded regions are crack surfaces. A and B are for loading in the 1 and 2 directions, respectively.*

Figures 3A and B show analysis coordinates for a single unit cell between cracks (which are indicated as shaded areas) in the three layers for loading in both the 1 (as done by Hashin) and 2 (added here) directions. To maximize overlap with Hashin's analysis, the direction 2 unit cell rotates material properties by 90˚. Each problem considers one half by symmetry defined by $0 \le z \le h = t_1 + t_2$ with $-a \le x \le a$ and $-b \le y \le b$ for direction 1, but $-b \le x \le b$ and $-a \le y \le a$ for direction 2. Note that the z axis for direction 2 is shifted from the centre to the left edge. With this shift, the layers labelled (1) and (2) retain the same orthotropic wood properties in the two unit cells — longitudinal, L, direction in y direction for layer (1) and x direction for layer (2) — and have cracks on the same surfaces. When the cracks are edges of timber elements, distances between the cracks ($2a$ and $2b$) are widths of timber in those layers. Most CLT will have layers of the same thickness ($2t_1 = t_2$) and us lumber of the same width ($2a = 2b$), but these parameters can be left as independent variables to keep the analysis more general.

Hashin's analysis [6] is too lengthy for this proceedings paper. Instead, the analysis procedure is outlined and complete results for calculations are provided. The reader is referred to Hashin's paper [6] and a longer CLT publication for analysis details [9]. Hashin wrote the components of total stress in layer (k) as:

$$\sigma_{ij}^{(k,tot)} = \sigma_{ij}^{(k,0)} + \sigma_{ij}^{(k)}$$

where $\sigma_{ij}^{(k,0)}$ is the stress in the corresponding CLT panel with no cracks and $\sigma_{ij}^{(k)}$ is the perturbation stress or change in stress due to addition of cracks. He derived a 3D admissible stress state for each layer [6], which can be generalized to account for direction i loading (i =1 or 2). The tensile stresses in the layers are

$$\sigma_{xx}^{(1)} = -\sigma_0 k_{xi}\phi_i(x) \qquad \sigma_{xx}^{(2)} = \frac{\sigma_0 k_{xi}\phi_i(x)}{\lambda_i}$$

$$\sigma_{yy}^{(1)} = -\sigma_0 k_{yi}\psi_i(y) \qquad \sigma_{yy}^{(2)} = \frac{\sigma_0 k_{yi}\psi_i(y)}{\lambda_i}$$

where σ_0 is uniaxial applied stress (in direction i), $\phi_i(x)$ and $\psi_i(y)$ are four unknown functions (two for each loading direction), $\lambda_1 = t_2/t_1$, and $\lambda_2 = t_1/t_2$. The stiffnesses, k_{xi} and k_{yi}, give the stress in layer 1 of a CLT with no cracks due to uniaxial load in direction i:

$$\sigma_{xx}^{(1,0)} = k_{xi}\sigma_0 \qquad \text{and} \qquad \sigma_{yy}^{(1,0)} = k_{yi}\sigma_0$$

where k_{xi} and k_{yi} are easily calculated from classical laminated plate theory [9,10] and are given in the appendix. The remaining 3D stresses (all shear stresses and normal stresses in the z direction) are given elsewhere [6,9]. The main simplifying assumptions are that $\sigma_{xx}^{(k)}$ depends only on x and $\sigma_{yy}^{(k)}$ depends only on y. Otherwise, the stress state is a valid admissible stress state. It satisfies all 3D equilibrium conditions, has zero shear on free surfaces and on midplanes of symmetry, has zero normal stress on free surfaces, and satisfies continuity of stresses as needed at layer interfaces.

Finally, the stresses satisfy all traction boundary conditions by virtue of the initial stress state and providing the unknown functions satisfy:

$$\phi_1(\pm a) = \psi_1(\pm b) = 1 \quad \phi_1'(\pm a) = \psi_1'(\pm b) = 0 \qquad (1)$$

$$\phi_2(\pm b) = \psi_2(\pm a) = 1 \quad \phi_2'(\pm b) = \psi_2'(\pm a) = 0 \qquad (2)$$

The function boundary conditions result in zero normal stress on all crack surfaces. Because shear stresses are proportional to function derivatives [6,9], the zero boundary conditions for derivatives gives zero shear stress on all crack surfaces.

The next step is to evaluate the total complementary energy in the unit cell. Because the stress state is admissible, one can then determine the best approximate stress state by minimizing that complementary energy. The minimization process, by using variational calculus, leads to coupled differential equations for the four unknown functions, which can be solved analytically using the boundary conditions in equations (1) and (2). The solutions are provided in the appendix.

2.1.1 In-Plane Tensile Moduli

By theorems of variational mechanics [6], the minimized complementary energy leads to lower bound moduli in the two directions as a function of crack spacings (a and b) in the layers [6,9]:

$$\frac{1}{E_{11}(a,b)} \le \frac{1}{E_{11}^0} + \frac{K_{x1}\langle\phi_1\rangle + K_{y1}\langle\psi_1\rangle}{1+\lambda_1} \qquad (3)$$

$$\frac{1}{E_{22}(a,b)} \le \frac{1}{E_{22}^0} + \frac{K_{x2}\langle\phi_2\rangle + K_{y2}\langle\psi_2\rangle}{1+\lambda_2} \qquad (4)$$

where superscript 0 indicates hypothetical CLT properties with no cracks and

$$K_{xi} = k_{xi}\left(\frac{k_{xi}(\lambda_i E_L + E_t) - 2k_{yi}E_t\nu_{Lt}(1+\lambda_i)}{\lambda_i E_L E_t}\right)$$

$$K_{yi} = k_{yi}\left(\frac{k_{yi}(E_L + \lambda_i E_t) - 2k_{xi}E_t\nu_{Lt}(1+\lambda_i)}{\lambda_i E_L E_t}\right)$$

where $\langle\phi_i\rangle$ and $\langle\psi_i\rangle$ are average values of those functions for loading direction i in the unit cell. E_L, E_t, and v_{Lt} are moduli and Poisson's ratio for the lumber in the plane of the CLT layers. L stands for longitudinal wood properties while t stands for property perpendicular to the grain direction and its direction in the wood will depend on the transverse grain pattern of the lumber (see sample grain patterns in figure 2 and the appendix for more details on wood property settings).

2.1.2 In-Plane Poisson's Ratio

Although it is not possible to place bounds on Poisson ratios, it is possible to calculate them using the above stress state. For direction 1 loading:

$$\nu_{12}(a,b) = -\frac{\langle\varepsilon_{22}\rangle}{\sigma_0}E_{11}(a,b)$$

where $\langle\varepsilon_{22}\rangle$ is average strain in the 2 direction. Hashin mistakenly equated this term to average strain over all layers [6], but that calculation does not account for extra strain resulting from crack opening displacements. After accounting for crack opening strain, $\langle\varepsilon_{22}\rangle$ can be derived as equal to average y direction strain in layer (1) only [9]. Finding this $\langle\varepsilon_{22}\rangle$ from the solved stress state (and a similar calculations for loading in direction 2), the in-plane Poisson's ratios are:

$$\frac{\nu_{12}(a,b)}{E_{11}(a,b)} = \frac{\nu_{12}^0}{E_{11}^0} + \frac{k_{y1}\langle\psi_1\rangle - \nu_{Lt}k_{x1}\langle\phi_1\rangle}{E_L} \qquad (5)$$

$$\frac{\nu_{21}(a,b)}{E_{22}(a,b)} = \frac{\nu_{21}^0}{E_{22}^0} + \frac{k_{y2}\langle\psi_2\rangle - \nu_{Lt}k_{x2}\langle\phi_2\rangle}{E_L} \qquad (6)$$

These two results are, as expected, identical and therefore satisfy standard relations between Poisson ratios.

2.1.3 Thermal and Moisture Expansion Coefficients

The usual approach to finding thermal expansion coefficients is to start over with a new stress analysis that explicitly includes residual stresses, but that work is not needed. Instead, thermal expansion coefficients of the CLT structure can be found from the Levin equation [11]:

$$\boldsymbol{\sigma}^{(m)} \cdot \boldsymbol{\alpha}_{eff} = \sum_i V_i \left\langle \boldsymbol{\sigma}^{(i,m)} \right\rangle \cdot \boldsymbol{\alpha}^{(i)}$$

where $\boldsymbol{\alpha}_{eff}$ is effective thermal expansion tensor of the composite. The sum is over phase i with volume fraction V_i and thermal expansion tensor $\boldsymbol{\alpha}^{(i)}$ where $\langle\boldsymbol{\sigma}^{(i,m)}\rangle$ is the average stress tensor in that phase due to any applied mechanical stresses $\boldsymbol{\sigma}^{(m)}$ (*i.e.*, the approximate stress state solutions). Applying this result to separate calculations using the direction 1 and 2 stress state solutions, the calculations leads to:

$$\alpha_1(a,b) = \alpha_L + \frac{\alpha_t - \alpha_L}{1+\lambda_1}\big(k_{x1}(1-\langle\phi_1\rangle) - k_{y1}(1-\langle\psi_1\rangle)\big)$$

$$\alpha_2(a,b) = \alpha_L + \frac{\alpha_t - \alpha_L}{1+\lambda_2}\big(k_{x2}(1-\langle\phi_2\rangle) - k_{y2}(1-\langle\psi_2\rangle)\big)$$

***Table** 1: Softwood lumber properties for CLT calculations. Moduli are in MPa and moisture expansion coefficients are % strain/% moisture content.*

Property	Value	Property	Value
E_L	8000	E_T	620
E_R	960	G_{LR}	800
G_{LT}	800	G_{RT}	80
ν_{LR}	0	ν_{LT}	0
ν_{RT}	0	β_L	0.0
β_R	0.16	β_T	0.26

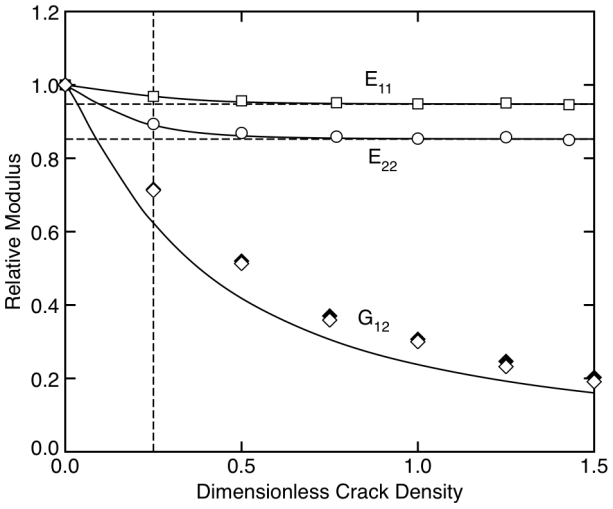

***Figure 4**: In-plane tensile and shear modulus by equations (solid lines) and by 3D MPM calculations (symbols). The filled symbols are for shear modulus with frictional contact on board edges. The dashed vertical line is as-made CLT crack density. The dashed horizontal lines and ply discount calculations.*

where α_L and α_t are the longitudinal and perpendicular in-plane thermal expansion coefficients of the wood (see appendix for details on wood properties). Note that the CLT expansion coefficients with no cracks (α_1^0 and α_2^0) are found using the above expressions by setting $\langle\phi_i\rangle$ and $\langle\psi_i\rangle$ to zero. This result is, as expected, identical to classical lamination theory approach to thermal expansion coefficients [10].

The analysis for moisture expansion coefficients, which may be more important for wood products, is identical and follows simply by replacing all thermal expansion coefficients (α) with the corresponding moisture expansion coefficients (β) for both the CLT panel and the wood.

3 RESULTS AND DISCUSSION

This section gives sample calculations for CLT properties as a function of crack spacings for three layer CLT made from flat-sawn lumber. The initial lumber cross section is 40 X 160 mm (1.57 X 6.30 in) and identical in all layers leading to $2t_1 = t_2 = 40$ mm and $a = b = 80$ mm. All results are plotted as a function of dimensionless crack density equal to $1/\rho_1 = a/t_1$ where ρ_1 is the aspect ratio of the lumber's cross-section. The as-made CLT has $1/\rho_1 = 40/160 = 0.25$ while zero crack density corresponds to CLT with no

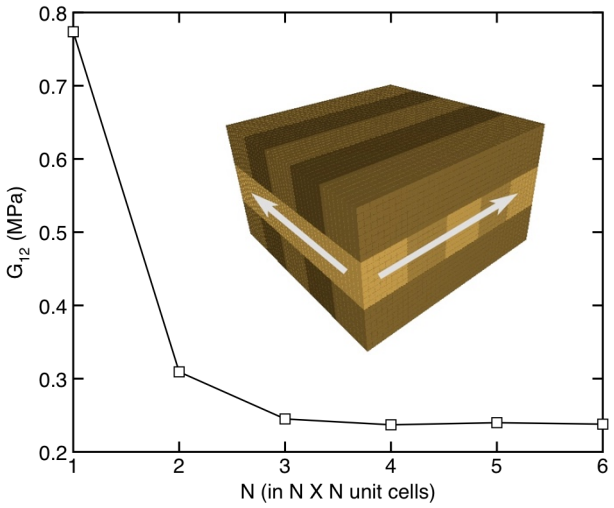

***Figure 5**: The in-plane shear modulus calculated using an MPM model with N X N units cells with a = b = 40 mm as a function of N. The graphic show 3D MPM model with 5 X 5 unit cells.*

cracks and $1/\rho_1 > 0.25$ corresponds to changes in properties caused by added cracks (as seen in figure 1). The assumed wood properties are in Table 1; for flat sawn lumber *t* and *r* in CLT correspond to *T* and *R* directions in the lumber.

Figure 4 plots the in-plane tensile moduli calculated by equations (3) and (4) and the results are normalized to moduli for CLT with no cracks. The vertical dashed line shows the as-made CLT while the horizontal dashed lines show the "ply-discount" limit for an infinite number of cracks. These moduli decrease as crack density increases. The ply discount limit corresponds to a calculation that assumes the 90˚ plies contribute zero stiffness to the panel. The reason tensile moduli decreases are modest is because of the high E_L/E_T ratio for wood. The 90˚ degree layers never contribute much stiffness and therefore when cracks form the degradation is rather small. The degradation would be slightly larger for radial-sawn lumber (because $E_R > E_T$).

The calculated moduli are formally lower bound predictions (*i.e.*, conservative) of the actual moduli. To check the utility of these lower bounds, the symbols show 3D material point method (MPM) calculations [13,14] for in-plane tensile moduli. The analytical and numerical results agree well demonstrating that the lower bounds are close to actual moduli.

Hashin's paper on orthogonally cracked composites mentions that "the problem of shearing of a cross-ply will be considered elsewhere." [6] Unfortunately, it turned out that the variational methods used for in-plane axial loading do not extend easily to in-plane shear loading. It is difficult to find an admissible stress state that is sufficiently robust to describe all 3D shear while also being simple enough for a closed-form, variational mechanics solution for shear modulus [15]. To provide complete results, this section quotes an alternate in-plane shear analysis method by Bogensperger *et al.* [16]. This analysis is a hybrid analytical/numerical result. It starts with a very simple model (*e.g.*, zero stiffness transverse to the plies

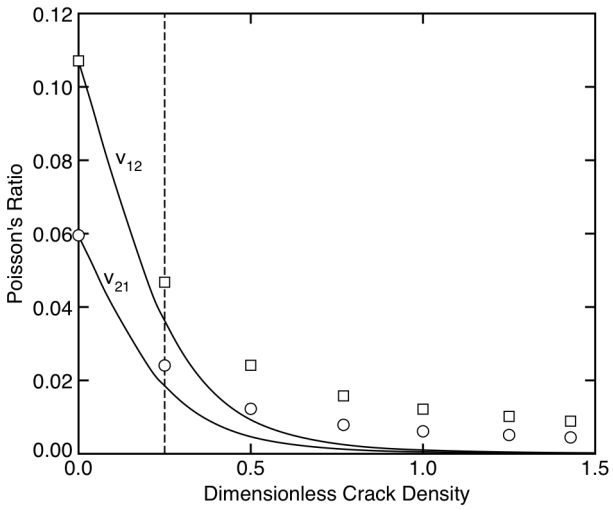

***Figure 6**: In-plane Poisson's ratios by equations (solid lines) and by 3D MPM calculations (symbols). The dashed vertical line is as-made CLT crack density.*

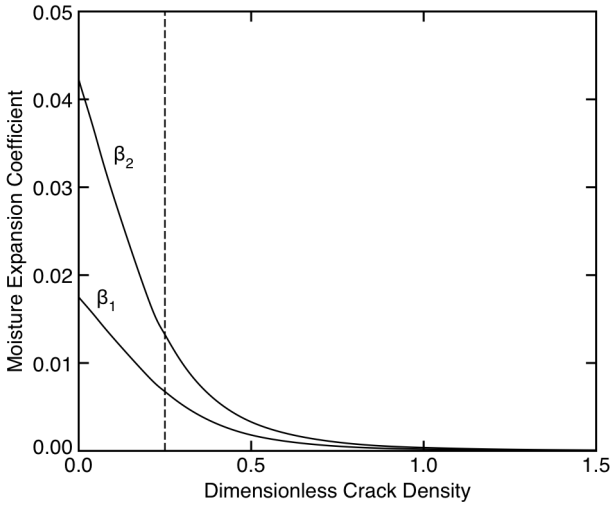

***Figure 7**: In-plane moisture expansion coefficients calculated by variational mechanics). The dashed vertical line is as-made CLT crack density.*

that is limited to CLT with constant board widths and constant thickness) and then calibrates the coefficients in this simplistic model using 3D finite element analysis (FEA). The resulting equation for three-layer CLT in current nomenclature is [16]:

$$G_{12}(a,a) = \frac{G_{Lt}}{1 + 3.207\rho_1^{-1.2053}} \tag{7}$$

where G_{Lt} is the in-plane shear modulus of the wood layers. This shear modulus result is compared to new 3D MPM calculations in figure 1. The agreement is reasonable with differences likely attributed to boundary conditions used in the FEA modelling in Ref. [16] compared to MPM modelling used here.

In MPM calculations here, attempts to model a single unit cell with shear force applied only to non-cracked surfaces only were not realistic The alternate approach used was to increase the size of the modelled CLT to include N X N unit cells and apply uniform shear on edges of the full structure. For large N, this approach is modelling a complete CLT panel. Analysis of multiple unit cells requires numerical methods that can handle sliding at interior non-glued edges but stick conditions on glued faces. Fortunately, MPM is capable of handling this issue [14]. Figure 5 shows shear modulus calculated from such an N X N unit cell model with $a = b = 40$ mm as a function of N. The results show that $N \geq 4$ is sufficiently large for numerical results to be representative of a full CLT panel. The shear modulus calculations in figure 4 used $N = 5$.

An interesting application of 3D MPM modelling of N X N unit cells is to investigate the role of friction between the edges. The filled symbols in figure 4 show numerical results for shear modulus when the coefficient of friction between wood edges is 0.3. In the presence of friction, the shear stiffness only slightly increased. One should not expect that frictional loading would significantly ameliorate the effects of non-glued edges or added cracks.

Figure 6 compares in-plain Poisson's ratios for a CLT panel (ν_{12} and ν_{21}) by modelling (equations (5) and (6) as curves) to 3D MPM calculations (symbols). The agreements are not as good as for moduli, but both results show that both Poisson's ratios approach zero as additional cracks are formed. Also note that the Poisson's ratios for as-made CLT (vertical line) are significantly different than the ratios calculated from a laminate theory that ignores cracks in the wood layers.

Figure 7 plots the moisture expansion coefficients for a CLT panel as a function of crack density (no modelling was done so curves are only for modelling predictions from section 2.1.3). Both moisture expansion coefficients approach zero as additional cracks are formed. Like Poisson's ratio, the moisture expansion coefficients for as-made CLT (vertical line) are significantly different than the results calculated from a laminate theory that ignores cracks in the wood layers. The modelling predictions for thermal expansion coefficients would be similar.

The fact that shear modulus, Poisson's ratio, thermal, and moisture expansion coefficients for CLT with initial cracks (based on lumber dimensions) are significantly different from simplified lamination models that ignore the cracks, suggests that property analysis of CLT panels should always account for those cracks. Ignoring the cracks may overestimate these properties by 100%.

3.1.1 Formation of Added Cracks

Potentially more important then initial CLT properties is how the properties will change in service. Changes in properties are expected because CLT will develop cracks and those additional cracks will change properties as shown in figure 4, 6, and 7. The properties that change the most are shear modulus, Poisson's ratios, and thermal and moisture expansion coefficients. In aerospace cross-laminated composites, it has been shown that the driving force for additional cracks is the total energy released due to the formation of each crack [1-4]. This key crack driving force can be calculated once effective mechanical and expansion properties are known.

Imagine an as-made CLT panel with lumber dimensions corresponding to $a = b = a_0$. If this panel is loaded in the

1 direction with stress σ_0, the first added crack will expected to form perpendicular to the wood grain in the (1) layer and form at the middle of one piece of lumber. This crack will change crack spacing from a_0 to $a_0/2$. From microcracking analysis in cross-laminated composites [1-4,17,18], the energy release rate (energy per unit crack area) for this added crack is:

$$G_{ac} = \frac{\left(\sigma_{xx}^{(1,0)}\right)^2 a_0 B}{2 t_1 k_{x1}^2} \left(\frac{1}{E_{11}(a_0/2, a_0)} - \frac{1}{E_{11}(a_0, a_0)} \right)$$

where $B = 2(t_1 + t_2)$ is total CLT thickness and

$$\sigma_{xx}^{(1,0)} = k_{x1}\sigma_0 + k_{th,1}\Delta T + k_{m,1}\Delta c$$

is the total stress in layer (1) for a CLT with no cracks. Importantly, this stress includes both applied load (σ_0) and residual stresses caused by changes in temperature (ΔT) or changes in moisture content (Δc). The new constants, $k_{th,1}$ and $k_{m,1}$ give residual stresses in layer (1). These terms are easily calculated from laminated plate theory [3] (but not given here). The next crack will form when G_{ac} exceeds the toughness, G_c, of the wood. For Douglas fir, the initiation toughness is about 200 J/m^2 [19].

The observation that CLT naturally forms additional cracks with minimal external load (*e.g.*, figure 1), suggests that the main driving forces for crack formation are residual stresses due to changes in moisture and temperature. The above energy release rate equation can be a tool for predicting the rate of formation of such cracks. The extension to further cracking would replace a_0 by the current crack spacing. The modelling of cracks in the outer layers would use a corresponding equation based on changes in $E_{22}(a,b)$ and crack spacing's in that layer. A robust approach to modelling durability of CLT panels should use these tools to account for the rate of formation of additional cracks and use the modelling to predict how those extra cracks will change all mechanical and expansion properties of the panel. This work will be addressed in a future publication.

3.1.2 Limitation and Future Work

The variational mechanics analysis presented above is limited to three layer CLT and to in-plane mechanical properties. Although the variational methods could be extended to more layers, the problem would involve a system of coupled equations that would likely need a numerical solution. Similarly, the variational methods could be used for laminates in bending [20,21], but only have a closed-form solution for three layer CLT.

A potential method to approximate CLT with any number of layers and to calculate bending and twisting properties is to use damage mechanics [22]. In this approach, a ply with cracks is replaced by a homogeneous ply with degraded properties. The degraded properties of a cracked wood layer could be evaluated by inverting an analysis for a three layer CLT with uncracked layers (see equations in the appendix) to solve for the effective layer properties required to match the variational mechanics results for mechanical properties as a function of the crack spacings in the layers. Once the effective properties are found, they could be input to classical laminated plate theory [10] to find CLT properties for any number of layers and to find laminate flexural properties.

Another limitation is that analysis is linear elastic. One non-linearity is the difference between tension and compression. The analysis assumes crack surfaces have zero normal stress, which is appropriate for tensile loading. During compression, however, the crack surfaces may come into contact and transmit normal stress (although would transmit shear stress only if sufficient friction). As a result, the compression moduli are likely to be higher than the tensile moduli. This effect would also affect bending calculations where some layers are in compression and others are in tension. Because cracks have a larger effect on tensile properties then on compression properties, the modelling used here can be claimed to give conservative predictions that would lead to fail-safe design. Those willing to rely on crack surface contact to provide structural integrity could potentially design to higher modulus values. Based on friction calculations in figure 4, however, crack surface contact likely has very little effect on shear modulus predictions.

The shear modulus predictions in equation (7) currently used a prior model that required numerical calibration [16]. A useful addition to CLT design would be a variational mechanics method to find a closed form solution for shear modulus in the presence of cracks. This solution has so far proved to be elusive.

Finally, durability analysis for CLT must account for the formation of additional cracks. Useful future work, therefore, would be experiments to monitor the rate of formation of additional cracks due to applied loads or to changes in temperature and moisture. These experiments could be analyzed by energy methods made possible by the property analyses in this paper. Once crack formation rates are known, durability could be predicted by modelling changes in structural integrity induced by the changes in properties caused by the additional cracks.

APPENDIX

The CLT properties were determined relative to the hypothetical CLT with no cracks. This structure would correspond to solid wood layers or approximately to CLT layers with glued edges before the formation of any added cracks. These properties can be found from classical laminated plate theory [9,10] applied to a laminate with an odd number, n, of alternating 0˚ and 90˚ layers with 0˚ plies on the surfaces and the laminate 1 direction in the L direction of the 0˚ plies. The results needed here are:

$$E_{11}^0 = \frac{Q_L R \nu_{Lt}}{\nu_{21}^0}(1 - \nu_{12}^0 \nu_{21}^0) \qquad Q_L = \frac{E_L}{1 - R\nu_{Lt}^2}$$

$$E_{22}^0 = \frac{Q_L R \nu_{Lt}}{\nu_{12}^0}(1 - \nu_{12}^0 \nu_{21}^0) \qquad G_{12}^0 = G_{Lt}$$

$$\nu_{12}^0 = \frac{2nR\nu_{Lt}}{(n-1) + R(n+1)} \qquad \nu_{21}^0 = \frac{\nu_{12}^0 E_{22}^0}{E_{11}^0}$$

where E_L and G_{Lt} are tensile and shear moduli of the lumber parallel to the grain, ν_{Lt} is the axial Poisson's ratio, and $R = E_t/E_L$ is ratio of tensile moduli in transverse and grain

directions. Note that E_t, G_{Lt}, and ν_{Lt} purposely used lowercase *t* to avoid confusion with tangential (*T*) direction of the wood. The actual values for these properties will depend on the end-grain pattern of the CLT lumber (see samples in figure 2). For example, with flat-sawn lumber, the *t* direction will approximately be the wood *T* direction ($E_t = E_T$) direction and wood radial (*R*) direction will be in the *z* direction. For radial sawn boards, the *t* direction will be in the *R* direction ($E_t = E_R$) with wood *T* direction in the *z* direction. For off-axis lumber (*e.g.*, lumber cut close to heartwood of the tree), E_t may be less then both E_T and E_R [12]. Although the analysis methods here could easily be modified to account for different properties in different layers, the results presented here assume identical or mean properties for all layers. Those properties can be chosen to reflect the most common end-grain patterns in the lumber. The use of *n* layers means these equations apply to any odd-ply structure such as plywood or CLT with more than three layers. The analytical results in this paper are for $n = 3$. The damage mechanics approach mentioned above provides one approximate method for generalizing to $n > 3$ [9].

Classical lamination theory also provides the constants for finding initial stresses in the layers:

$$k_{x1} = \frac{Q_L(1-\nu_{Lt}\nu_{12}^0)}{E_{11}^0} \quad k_{x2} = \frac{Q_L(1-\nu_{Lt}\nu_{21}^0)}{E_{22}^0}$$

$$k_{y1} = \frac{Q_L(R\nu_{Lt}-\nu_{12}^0)}{E_{11}^0} \quad k_{y2} = \frac{Q_L(R\nu_{Lt}-\nu_{21}^0)}{E_{22}^0}$$

Lastly, we need to minimize the complementary energy to find the unknown $\phi_i(x)$ and $\psi_i(y)$. These functions are found by solving coupled differential equations, which can be solved in closed form [6,9]. The solutions are best expressed in terms of constants defined from the wood properties. For loading in the $i = 1$ direction, the needed constants are:

$$A_0 = \frac{1}{E_t} + \frac{1}{\lambda_i E_L} \qquad B_0 = -\frac{\nu_{Lt}(1+\lambda_i)}{\lambda_i E_L}$$

$$C_0 = \frac{1}{E_L} + \frac{1}{\lambda_i E_t} \qquad A_1 = \frac{1}{3G_{RT}} + \frac{\lambda_i}{3G_{Lr}}$$

$$B_1 = \frac{1}{3G_{Lr}} + \frac{\lambda_i}{3G_{RT}} \quad A_2 = \frac{(3\lambda_1+2)\nu_{tr}}{3E_t} - \frac{\lambda_1\nu_{Lr}}{3E_L}$$

$$B_2 = \frac{(3\lambda_1+2)\nu_{Lr}}{3E_L} - \frac{\lambda_1\nu_{tr}}{3E_t}$$

$$C_2 = \frac{(\lambda_1+1)(3\lambda_1^2+12\lambda_1+8)}{60E_r}$$

For loading in the 2 direction, use $i = 2$ in the first five constants and replace the last three constants by:

$$A_2' = \frac{(2\lambda_2+3)\nu_{Lr}}{3E_L} - \frac{\nu_{tr}}{3E_t}$$

$$B_2' = \frac{(2\lambda_2+3)\nu_{tr}}{3E_t} - \frac{\nu_{Lr}}{3E_L}$$

$$C_2' = \frac{(\lambda_2+1)(8\lambda_2^2+12\lambda_2+3)}{60E_r}$$

For each loading direction *i*, the function $\phi_i(\xi)$ (where $\xi = x/t_i$) is determined using the above constants and new constants derived from the characteristic equation for the controlling differential equations [6,9]:

$$p_1 = \frac{A_2 - A_1}{C_2} \quad q_1 = \frac{A_0}{C_2} \quad p_2 = \frac{B_2 - B_1}{C_2} \quad q_2 = \frac{C_0}{C_2}$$

$$m_1 = \frac{k_{yi}}{k_{xi}}\frac{B_0}{A_0} \qquad m_2 = \frac{k_{xi}}{k_{yi}}\frac{B_0}{C_0}$$

but A_2, B_2, and C_2 are replaced by A_2', B_2', and C_2 for loading in direction 2. All combinations of CLT properties have $p_i < 0$ and $q_i > 0$, but the final solution depends on their relative values. When $4q_1 > p_1^2$:

$$\phi_i(\xi) = \big(1 + m_1\langle\psi_i\rangle\big)\big(D_1\cosh(\alpha\xi)\cos(\beta\xi) + D_2\sinh(\alpha\xi)\sin(\beta\xi)\big) - m_1\langle\psi_i\rangle$$

where

$$D_1 = \frac{2\big(\alpha\cosh(\alpha\rho_1)\sin(\beta\rho_1) + \beta\sinh(\alpha\rho_1)\cos(\beta\rho_1)\big)}{\beta\sinh(2\alpha\rho_1) + \alpha\sin(2\beta\rho_1)}$$

$$D_2 = \frac{2\big(\beta\cosh(\alpha\rho_1)\sin(\beta\rho_1) - \alpha\sinh(\alpha\rho_1)\cos(\beta\rho_1)\big)}{\beta\sinh(2\alpha\rho_1) + \alpha\sin(2\beta\rho_1)}$$

$$\alpha, \beta = \frac{1}{2}\sqrt{2\sqrt{q_1} \mp p_1}$$

and $\rho_1 = a/t_1$. The average value of $\phi_i(\xi)$ is

$$\langle\phi_i\rangle = \big(1 + m_1\langle\psi_i\rangle\big)\omega_1 - m_1\langle\psi_i\rangle \tag{A1}$$

where

$$\omega_1 = \frac{2\alpha\beta\big(\cosh(2\alpha\rho_1) - \cos(2\beta\rho_1)\big)}{\rho_1(\alpha^2+\beta^2)\big(\beta\sinh(2\alpha\rho_1) + \alpha\sin(2\beta\rho_1)\big)}$$

When $4q_1 > p_1^2$:

$$\phi_i(\xi) = \big(1 + m_1\langle\psi_1\rangle\big)\big(D_1\cosh(\alpha\xi) + D_2\cosh(\beta\xi)\big) - m_1\langle\psi_i\rangle$$

where

$$D_1 = \frac{-\beta\sinh(\beta\rho_1)}{\alpha\sinh(\alpha\rho_1)\cosh(\beta\rho_1) - \beta\cosh(\alpha\rho_1)\sinh(\beta\rho_1)}$$

$$D_2 = \frac{\alpha\sinh(\alpha\rho_1)}{\alpha\sinh(\alpha\rho_1)\cosh(\beta\rho_1) - \beta\cosh(\alpha\rho_1)\sinh(\beta\rho_1)}$$

$$\alpha, \beta = \sqrt{-\frac{p_1}{2} \pm \sqrt{\frac{p_1^2}{4} - q_1}}$$

The average value of $\phi_i(\xi)$ is the same as equation (A1) except now

$$\omega_1 = \frac{(\alpha^2-\beta^2)\sinh(\alpha\rho_1)\sinh(\beta\rho_1)}{\rho_1\alpha\beta\big(\alpha\sinh(\alpha\rho_1)\cosh(\beta\rho_1) - \beta\cosh(\alpha\rho_1)\sinh(\beta\rho_1)\big)}$$

To find $\psi_i(\eta)$, use the above equations but replace $\phi_i(\xi)$, p_1, q_1, ρ_1, m_1, $\langle\psi_i\rangle$, ω_1, and ξ with $\psi_i(\eta)$, p_2, q_2, $\rho_2 = b/t_2$, m_2, $\langle\phi_i\rangle$, ω_2, and $\eta = y/t_i$, respectively and note that α and

β will be different. Note that equation (A1) will now involve ω_2 and the subsequent equation for ω_1 now defines the needed ω_2.

All effective properties depend on the average values $\langle\phi_i\rangle$ and $\langle\psi_i\rangle$. To find these terms, solve equation (A1) and the corresponding equation for $\langle\psi_i\rangle$ to get:

$$\langle\phi_i\rangle = \frac{\omega_1 - m_1\omega_2(1-\omega_1)}{1 - m_1 m_2(1-\omega_1)(1-\omega_2)}$$

$$\langle\psi_i\rangle = \frac{\omega_2 - m_2\omega_1(1-\omega_2)}{1 - m_1 m_2(1-\omega_1)(1-\omega_2)}$$

where ω_1 and ω_2 are determined from the appropriate form for $\phi_i(\xi)$ and $\psi_i(\eta)$ in the previous equations. Repeating this calculation for both loading directions determines all terms need to find all mechanical properties for a three-layer CLT panels.

REFERENCES

[1] J. A. Nairn. The strain energy release rate of composite microcracking: A variational approach. *J. Comp. Mat.*, **23**:1106–1129, 1989.

[2] J. A. Nairn, S. Hu, and J. S. Bark. A critical evaluation of theories for predicting microcracking in composite laminates. *J. Mat. Sci.*, **28**:5099–5111, 1993.

[3] J. A. Nairn and S. Hu. Micromechanics of Damage: A Case Study of Matrix Microcracking, chapter in: *Damage Mechanics of Composite Materials*, pages 187–243. Elsevier, Amsterdam, 1994.

[4] J. A. Nairn. Matrix Microcracking, chapter in: *Composites, volume 2 of Comprehensive Composite Materials*, pages 403–432. Elsevier Science, 2000.

[5] Z. Hashin. Analysis of cracked laminates: A variational approach. *Mech. of Mat.*, **4**:121–136, 1985.

[6] Z. Hashin. Analysis of orthogonally cracked laminates under tension. *J. Appl. Mech.*, **54**:872–879, 1987.

[7] Z. Hashin. Thermal expansion coefficients of cracked laminates. *Comp. Sci. & Tech.*, **31**:247–260, 1988.

[8] S. R. Frost. The impact behaviour and damage tolerance of filament would glass fibre/epoxy matrix pipes. *6th Int. Conf. of Fiber-Reinforced Composites*, **3**:1–10, University of Newcastle Upon Tyne, March 29-31, 1994.

[9] J. A. Nairn, Mechanics of Cross Laminated Timber Accounting for Non-Glued Edges and Additional Cracks, in preparation (2016).

[10] R. M. Jones. *Mechanics of Composite Materials*. Scripta Book Company, Washington, DC, 1975.

[11] V. M. Levin. On the coefficients of thermal expansion in heterogeneous materials. *Mechanics of Solids*, **2**:58–61, 1967.

[12] J. A. Nairn. A numerical study of the transverse modulus of wood as a function of grain orientation and properties. *Holzforschung*, **61**:406–413, 2007.

[13] J. A. Nairn. Material point method (NairnMPM) and finite element analysis (NairnFEA) open-source software. http://osupdocs.forestry.oregonstate.edu/index.php/Main Page, 2016.

[14] J. A. Nairn. Modeling of imperfect interfaces in the material point method using multimaterial methods. *Computer Modeling in Eng. & Sci.*, **92**(3):271–299, 2013.

[15] Z. Hashin, personal communication, 2010.

[16] T. Bogensperger, T. Moosbrugger, and G. Silly, Verification of CLT-plates under loads in plane. *World Conference on Timber Engineering,* Riva del Garda, Italy, 20-24 June, 2010.

[17] J. A. Nairn. Fracture mechanics of composites with residual thermal stresses. *J. Appl. Mech.*, **64**:804–810, 1997.

[18] J.A. Nairn. Finite fracture mechanics of matrix microcracking in composites. In *The Application of Fracture Mechanics to Polymers, Adhesives and Composites,* ed. D. R. Moore, Elsevier Science, London, UK, 2004.

[19] N. Matsumoto and J. A. Nairn. Fracture toughness of wood and wood composites during crack propagation. Wood and Fiber Science, **44**(2):121–133, 2012.

[20] S. R. Kim and J. A. Nairn. Fracture mechanics analysis of coating/substrate systems subjected to tension or bending loads I: Theory. *Engr. Fract. Mech.*, **65**:573–593, 2000.

[21] S. R. Kim and J. A. Nairn. Fracture mechanics analysis of coating/substrate systems subjected to tension or bending loads II: Experiments in bending. *Engr. Fract. Mech.*, **65**:595–607, 2000.

[22] J.-L. Chaboche. Development of continuum damage mechanics for elastic solids sustaining anisotropic and unilateral damage. *International Journal of Damage Mechanics,* **2**(4):311–329, 1993.